Available online at www.eccomasproceedia.org
Eccomas Proceedia COMPDYN (2023) 1169-1176

ECCOMAS Proceedia

COMPDYN 2023
9th ECCOMAS Thematic Conference on
Computational Methods in Structural Dynamics and Earthquake Engineering
M. Papadrakakis, M. Fragiadakis (eds.)
Athens, Greece, 12-14 June 2023

SURROGATE MODELING OF THE RESPONSE OF A BEARING DEVICE FOR PASSIVE SEISMIC ISOLATION

Todor Zhelyazov[1]

[1] Technical University of Sofia
8, Kliment Ohridski blvd, Sofia, 1000, Bulgaria
e-mail: elovar@yahoo.com

Abstract

The contribution discusses the application of a multilayer perceptron network in the assessment of the behavior of bearing devices for passive seismic isolation. One of the essential characteristics of a bearing device is the relationship between the applied displacement and the restoring force. Besides the relationship between the applied displacement and the generated restoring force, an extra equation characterizing the evolution of the hysteresis variable is commonly provided. A neural network comprising an input layer, several hidden layers, and an output layer is built to reproduce the nonlinear constitutive relationship for the sliding isolator. The neural network is to be trained to reproduce the response of the bearing device considered separately, i.e., the device response in a characterization test. An accent in the study is on the use of synthetic data for the perceptron's training as an alternative to using data sets using results obtained by finite element analysis or experimental studies.

Keywords: Passive seismic isolation, Modeling, Analytic models, Multilayer perceptron.

doi: 10.7712/120123.10466.20481

1 INTRODUCTION

Friction pendulum (FP) systems are among the most widely used technologies for seismic isolation. Typically, such an isolator consists of a sliding concave spherical surface in stainless steel, a steel slider, and an upper steel plate with a housing for the slider. A polymer composite liner is placed on the housing and the lower surface of the slider to facilitate sliding.

This type of isolator is characterized by a large displacement capacity, limited only by its in-plane geometric dimensions. Moreover, the period of vibration of a base-isolated structure equipped with FP isolators is primarily controlled by the radius of the concave sliding surface, and not on the supported mass [1], [2]. Compared to other frequently used isolators, the Lead-Core Rubber Bearings, the dissipation capacity of sliding isolators is lower; on the other hand, the FP systems are more compact with a considerably lower height, which makes them suitable for retrofit applications [3].

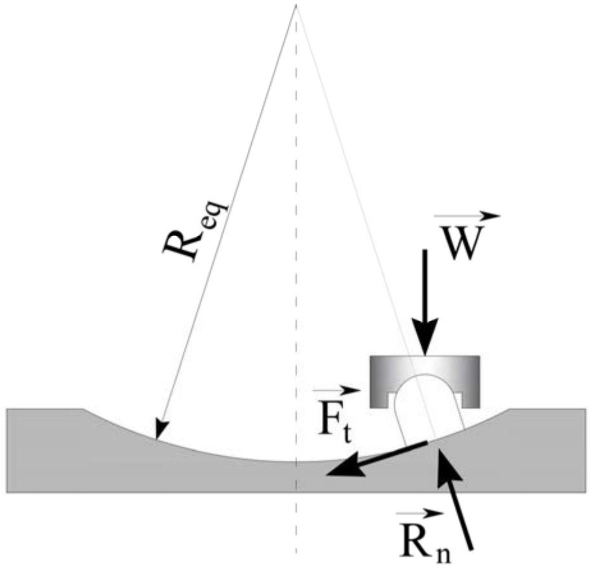

Figure 1: Simplified scheme of the displaced position of the seismic isolator.

A schematization of the forces acting on the slider (Figure 1) includes the weight of the superstructure **W**, the reaction normal to the concave sliding surface $\mathbf{R_n}$, and $\mathbf{F_t}$ - a force generated during the sliding. $\mathbf{F_t}$ can be thought of as a vector situated in the tangent plane, at the current position of the slider and, by assumption, depends on the instantaneous value of the friction coefficient.

For example, a finite element model provides a detailed output. However, the computational cost might hinder its implementation in the dynamic response analysis of a base-isolated structure. In this context, light, analytical models appear as a competitive alternative.

The article investigates the application of machine learning algorithms, and, more precisely, of multilayer perceptrons, to predict the behavior of FP isolators. The target data sets needed for the training algorithm can be obtained either by previously reported experimental investigations, results obtained by finite element analysis, or synthetic data. Often, the empirically obtained database might be limited by the number of conducted experiments, and the number of samples might be small compared to the number of model features. Clearly, this is attributed to the fact that experimental investigation might be and often is extremely resource-demanding. Also, in the reported experimental investigations, there might be missing data with respect to the input required by the assumed model. As previously discussed, finite element simulations can also be demanding in computational resources. Synthetic data can come in handy to fill possible gaps in the definition of the space devoted to multilayer perceptron training. Synthetic data can be easily obtained using widely accepted analytical models. It should be noted that although providing target data points, analytical models are not involved by any means in the multilayer perceptron algorithm.

2 ANALYTICAL MODELING

The 'force-displacement' relationship according to Figure 1 (see also [4])

$$F_t = \frac{W}{R_{eqv}} u + \mu W sign\left(\dot{u}\right) \tag{1}$$

where **W** is the vertical load carried by the bearing device, R_{eqv} is the radius of the concave sliding surface defined based on the geometry of the sliding isolator, u is the current displacement, μ is the friction coefficient, $\dot{u}$ is the time derivative of the displacement vector, and $sign\left(\dot{u}\right)$ denotes the signum function. More sophisticated constitutive relationships for the interface ([5], [6]) take into account the hysteresis variable, defined based on viscoplasticity models

$$\begin{pmatrix} \dot{Z}_x d_Y \\ \dot{Z}_y d_Y \end{pmatrix} = \begin{pmatrix} A\dot{U}_x \\ A\dot{U}_y \end{pmatrix} - \begin{bmatrix} Z_x^2 \left(\gamma.sign\left(\dot{U}_x Z_x\right) + \beta\right) & Z_x Z_y \left(\gamma.sign\left(\dot{U}_y Z_y\right) + \beta\right) \\ Z_x Z_y \left(\gamma.sign\left(\dot{U}_x Z_x\right) + \beta\right) & Z_y^2 \left(\gamma.sign\left(\dot{U}_y Z_y\right) + \beta\right) \end{bmatrix} \begin{pmatrix} \dot{U}_x \\ \dot{U}_y \end{pmatrix} \tag{2}$$

where Z_x and Z_y are hysteresis variables for local X- and Y- directions, d_Y is the yield displacement, A, γ, β are model parameters. Under some conditions (please, refer to [5]), it can be found that

$$\begin{aligned} Z_x &= \cos\left(\theta\right) \\ Z_y &= \sin\left(\theta\right) \end{aligned} \tag{3}$$

where $\theta = \arctan\left(\frac{\dot{U}_y}{\dot{U}_x}\right)$, $\dot{U}_x$ and $\dot{U}_y$ are the vector velocity components derived from the displacement vector. Thus, according to [7], for a sliding bearing, assuming isotropic sliding, the sliding forces components are

$$\begin{aligned} F_x &= \mu.W.Z_x \\ F_y &= \mu.W.Z_y \end{aligned} \tag{4}$$

In equations (4), μ denotes the friction coefficient and W is the vertical load transferred to the bearing device.

According to the current state of knowledge, the friction coefficient depends on the sliding velocity (v), on the vertical load transferred from the superstructure (W), and on the temperature (T), given that the temperature rises during sliding. The descriptive models have evolved from relationships that do not take into account the rise in the temperature (see, for example, [7]) to empirical relationships which assess the effects due to the sliding velocity, the vertical load, and the temperature separately and then combine them [8]

$$\mu = f\left(v\right).f\left(W\right).f\left(T\right) \tag{5}$$

The contribution of the sliding velocity, normal pressure and temperature are evaluated

$$f\left(v\right)=v_0+\left(1-v_0\right)\exp\left(-\left|v\right|/v_{ref}\right) \tag{6}$$

$$f\left(W\right)=\mu_0\exp\left(-W/W_{ref}\right) \tag{7}$$

$$f\left(T\right)=\exp\left(-\left(\frac{C}{C_{ref}}\right)^{\beta}\right) \tag{8}$$

In equations (6)-(8) v_0, v_{ref}, N_{ref}, C_{ref}, and β are model parameters.

As an example, for imposed in-plane displacements according to Figure 2 and Figure 3,

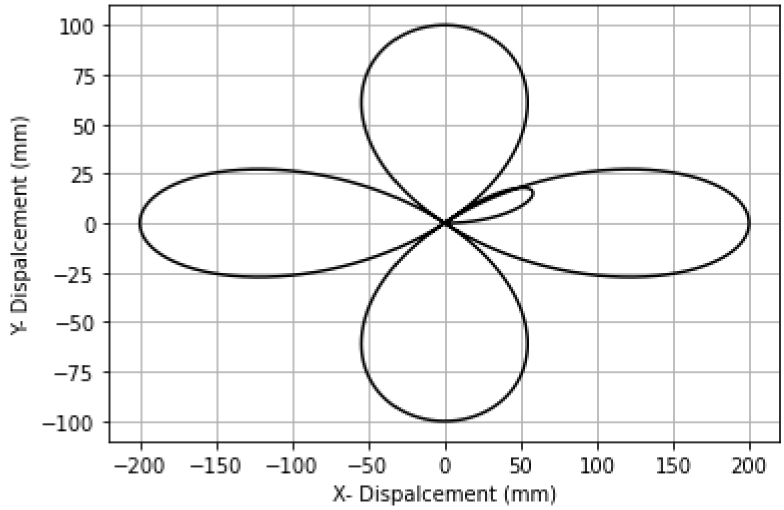

Figure 2: In-plane displacements resolved in X- and Y- components applied to the sliding isolator.

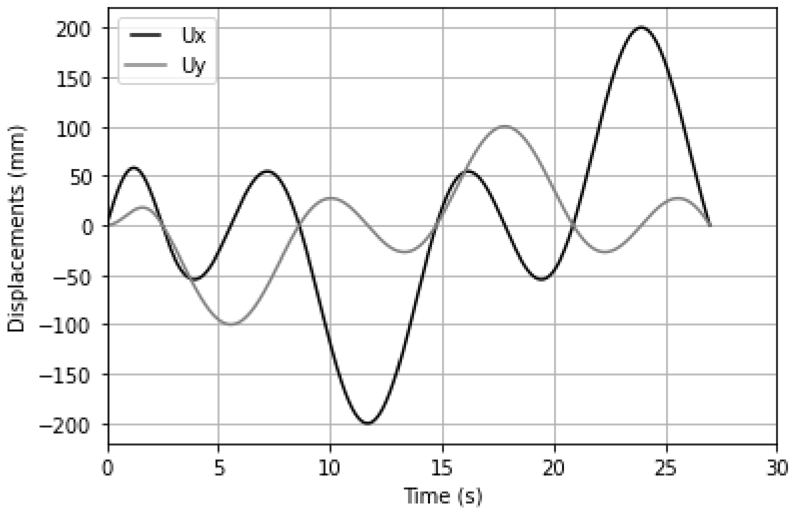

Figure 3: The time evolution of the applied in-plane displacements' X- and Y- components.

the 'generated force - displacement' relationship, in longitudinal and transverse directions, based on equations (1)-(8), can be obtained (as shown in Figure 4 and Figure 5).

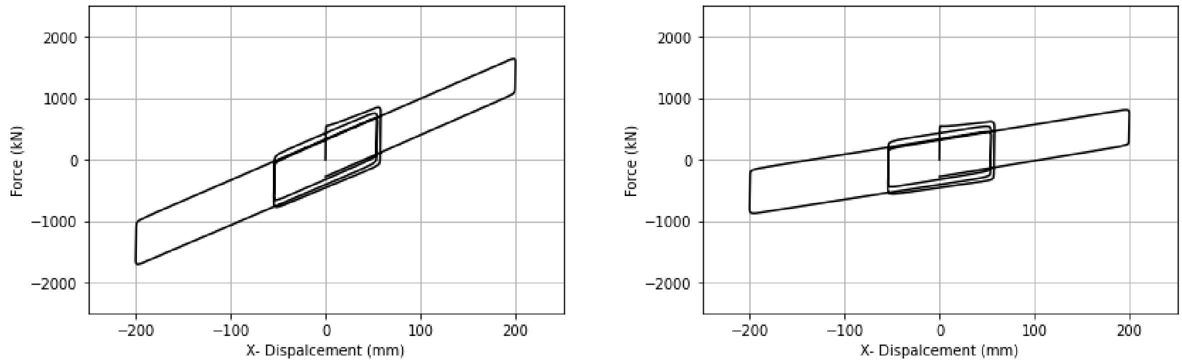

Figure 4: Analytically relationship between the x-component of the applied displacement and the x-component of the force generated in the isolator for R_{eqv}=950 mm (a); R_{eqv}=2450 mm (b).

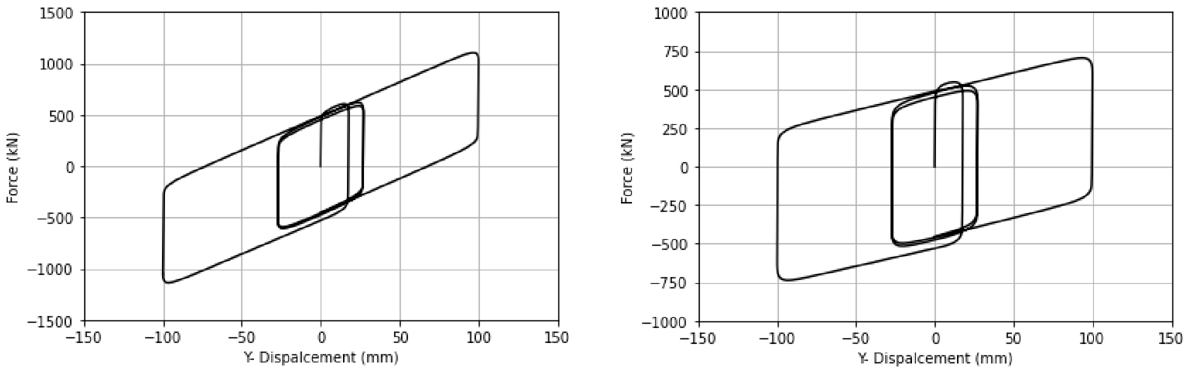

Figure 5: Analytically relationship between the y-component of the applied displacement and the y-component of the force generated in the isolator for R_{eqv}=950 mm (a); R_{eqv}=2450 mm (b).

3 ASSESSEMENT OF THE GLOBAL BEHAVIOR

The numerically obtained 'force-displacement' relationships can provide data points for the multilayer perceptron training or the identification of some characteristics defining the overall behavior of the isolator. The macroscopic response of the bearing device is characterized by the effective stiffness (K_{eff}), the Energy Dissipated by Cycle (EDC) in the hysteresis loop, and the effective damping (ξ_{eff}). The effective stiffness and the dissipated energy can be obtained according to [9]

$$K_{eff} = \frac{\left(\left|F_i^+\right| + \left|F_i^-\right|\right)}{\left(\left|\Delta_i^+\right| + \left|\Delta_i^-\right|\right)} \tag{9}$$

$$EDC = \int_{u_{\min}}^{u_{\max}} \left(F_i^+\left(u\right) - F_i^-\left(u\right)\right) du \tag{10}$$

while the effective damping can be evaluated following [10], [11].

$$\xi_{eff} = \frac{2}{\pi} \frac{\mu}{\mu + \dfrac{A_u}{R}} \tag{11}$$

4 MULTILAYER PERCEPTRON

The multilayer perceptron, employed as an approximator, can provide either an estimate of the generated force-displacement relationship typically used to characterize the response of the bearing device or a reduction of some parameter quantifying the overall behavior of the isolator. In both cases, the multilayer perceptron can be fed with experimental results, results obtained by finite element simulations, and synthetic data. The latter option can be implemented using the algorithm defined in equations (1)-(8).

The multilayer perceptron consists of an input layer, several hidden layers, and an output layer. Figure 6 presents a conceptual image of the neural network consisting of one input layer containing k neurons, several hidden layers of the same length (n neurons each), and an output layer.

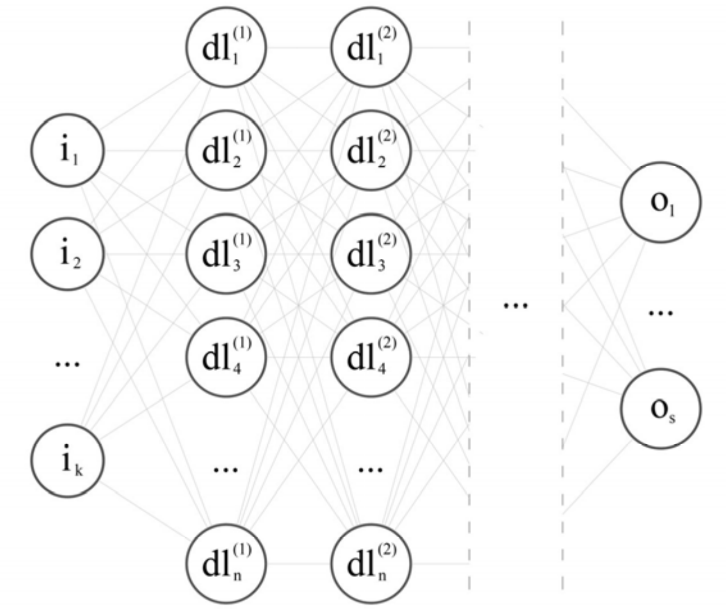

Figure 6: A sample multilayer perceptron.

The layers are initially designed as ‘dense’ with a presumed option for regularization. The Rectified Linear Unit (ReLU) activation function is used for the hidden layer. The argument of the ReLU function is defined as follows

$$x = w^T.z + b \tag{12}$$

where w^T is an array (transposed) containing the weights of the connections to a given neuron, z is an array containing the outputs from the neurons in the previous layer, $w^T.z$ is the dot product of w^T and z, and b is the bias associated with the considered neuron. The activation function itself is classically defined

$$\mathrm{Re}LU(x) = \begin{cases} 0 & if \quad x < 0 \\ x & if \quad x \geq 0 \end{cases} \tag{13}$$

Figure 7 depicts a neuron $dl_j^{(i)}$ (from the hidden layer i) which takes n $z_p^{(i-1)}$, $(p=1...n)$ inputs from the neurons of the previous layer, as each connections has a weight w_p. The neuron provides an output $z_j^{(i)}$.

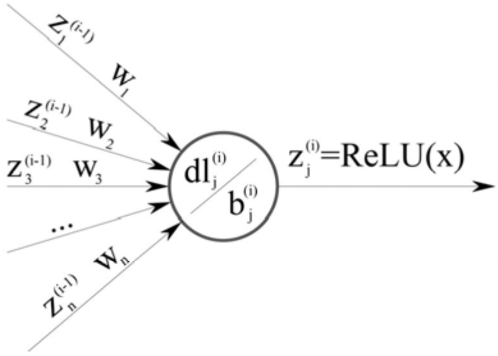

Figure 7: Operations in a neuron that belongs to a hidden dense layer.

The hyperparameters of the multilayer perceptron (such as the learning rate and the number of epochs) are to be chosen in a way allowing to obtain an optimal behavior of the neural network. Alternatively, an automated Bayesian algorithm can be employed. The training of the multilayer perceptron is based on the Mean Squared Error (MSE) algorithm

$$F = \frac{1}{N}\sum_{s=1}^{N}\left(o_i - \widehat{o}_i\right)^2 . \tag{14}$$

where o_i is the output provided and, is the desired (i.e., targeted) value, and N is the number of data points where the output is estimated. Target values can be provided either by using experimental results, results obtained by finite element analysis or synthetic data. The minimization of the mean squared error corresponds to the maximization of the likelihood estimate presuming Gaussian distribution.

5 CONCLUSIONS

The implementation of a multilayer perceptron in the analysis of the behavior of a sliding bearing for base-isolated structures has been discussed. The neural network consists of one input layer, several hidden dense layers equipped with a ReLU activation function, and an output layer. The influence of some parameters of the network's architecture (the number of layers and the number of neurons per layer) and the hyperparameters (the learning rate and the number of epochs) is being manually investigated to obtain optimal performance of the multilayer perceptron.

The focus of the reported study is on the definition of the data set to be used for the training and the subsequent validation of the perceptron. Compared with a detailed finite element model, for example, the neuron network will possibly enable the simulation of the behavior of a device for passive seismic isolation within a base-isolated structure at a reasonable computational cost.

Synthetic data has been employed for the training. Widely accepted analytical models have been implemented to generate the target data sets. It should be noted that the analytical model itself is not an element of the neural network architecture. Alternative options to provide data needed for the target (or the validation) data set are empirical data (for example, experimental studies reported in the literature) or data obtained by finite element analysis.

The hypothesis can be formulated that, upon proper training based on the simulation of the mechanical and the thermo-mechanical responses of the sliding isolator obtained in the characterization test, the multilayer perceptron might be capable of predicting the behavior of the bearing in more complex loading conditions, such as those that could arise in a base-isolated structure.

REFERENCES

[1] V.A. Zayas, S.S. Low, S.S. Mahin, *The FPS earthquake resisting system* [Report no. CB/EERC-87/01]. Berkeley: Earthquake Engineering Research Center, University of California, 1987.

[2] A. Mokha, M.C. Constantinou, A.M. Reinhorn, V.A. Zayas, Experimental study of friction-pendulum isolation system, *Journal of Structural Engineering (US)*, **117**(4), 1201-1217, 1991.

[3] A.S. Mokha, N. Amin, M.C. Constantinou, V. Zayas, Seismic isolation retrofit of large historical building, *Journal of Structural Engineering*, **122**(3), 298-308, 1996.

[4] J.L Almazan, J.C. De la Llera, J.A. Inaudi, Modeling aspects of structures isolated with the friction pendulum system. Earthquake Eng. Struct. Dyn., **27**, 845–867, 1998

[5] M. Constantinou, A. Mokha, A. Reinhorn, Teflon bearings in base isolation. II: modeling, *Journal of Structural Engineering*, **116**(2), 455-474, 1990.

[6] Y.J. Park, Y.K Wen, A. H-S. Ang, Random vibrations of hysteretic system under a bi-directional ground motion, *Earthquake Engineering and Structural Dynamics*, **14**(4), 543-557, 1986.

[7] S. Nagarajaiah, A.M. Reinhorn, M.C. Constantinou. Nonlinear dynamic analysis of 3-d-base-isolated structures. *Journal of Structural Engineering New York*, **117**(7), 2035–2054, 1991.

[8] G. Lomiento , N. Bonessio, G. Benzoni, Friction Model for Sliding Bearings under Seismic Excitation, Journal of Earthquake Engineering, **17**(8), 1162-1191, 2013

[9] Q. Han, J. Wen, Z. Zhong, X. Du, Numerical Simulation of Frictional Heating Effects of Sliding Friction Bearings for Isolated Bridges. *International Journal of Structural Stability and Dynamics*, **18**(08), 1840008, 2018.

[10] V.A. Zayas, S.S. Low, S.A. Mahin, A simple pendulum technique for achieving seismic isolation, *Earthquake Spectra*, **6**(2), 317–334, 1990.

[11] V. Quaglini, M. Bocciarelli, E. Gandelli, P. Dubini Numerical Assessment of Frictional Heating in Sliding Bearings for Seismic Isolation, Journal of Earthquake Engineering, **18**(8), 1198-1216, 2014.